MDPI

Article

Spatial-Temporal Evolution Characteristics and Driving Force Analysis of NDVI in the Minjiang River Basin, China, from 2001 to 2020

Junyi Wang, Yifei Fan, Yu Yang, Luoqi Zhang, Yan Zhang, Shixiang Li and Yali Wei *

College of Resource, Sichuan Agricultural University, Chengdu 611130, China
* Correspondence: weiyali@sicau.edu.cn

Abstract: Monitoring vegetation growth and exploring the driving force behind it is very important for the study of global climate change and ecological environmental protection. Based on Normalized Difference Vegetation Index (NDVI) data from Moderate-Resolution Imaging Spectroradiometer (MODIS), meteorological and nighttime lights data from 2001 to 2020, this study uses the Theil–Sen slope test, Mann–Kendall significance test, Rescaled Range Analysis and partial correlation analysis to investigate the evolution of NDVI in the Minjiang River Basin, China, from three aspects: the spatial-temporal variation characteristics and future trend prediction of NDVI, the variation of climate and human activities in the basin, and the influences of different driving forces on NDVI. The results show that the average NDVI in the growing season was 0.60 in the Minjiang River Basin in the past twenty years, with a growth rate of 0.002/a. The area with high NDVI growth accounts for 66.02%, mainly distributed in the southeast, the central and the northern low-altitude areas of the basin. Combined with the Hurst index, the NDVI in the Minjiang River Basin exhibits an anti-sustainable tendency, with 63.22% of the area changing from improvement to degradation in the future. Meanwhile, the spatial differentiation of NDVI in the Minjiang River Basin is mainly affected by topography and climate factors, followed by human activities. This study not only provides scientific guidelines for the vegetation restoration, soil and water conservation and sustainable development of the Minjiang River Basin, but also provides a scientific basis for making informed decisions on ecological protection under the impacts of climate change and human activities.

Keywords: Minjiang River Basin; NDVI; correlation analysis; driving force

1. Introduction

Vegetation is a significant indicator of global climate change. The relationship between vegetation and global change has become a major concern [1,2]. The Normalized Difference Vegetation Index (NDVI), one of the earliest remote sensing analytical products for simplifying the complexity of multi-spectral imagery, has been considered an effective indicator for monitoring terrestrial vegetation changes [3–7]. The NDVI has a linear or near-linear relationship with leaf density, photosynthetic effective radiation and vegetation productivity, and is one of the most used indices for investigating the growth status and vegetation coverage [8,9]. Studies have shown that vegetation activity shows an increase in global variation [10], while the NDVI in many parts of Eurasia showed some degree of decline after the mid-1990s [11]. Since the 1980s, the vegetation cover during the growing season in China has shown a significant increasing trend, but this trend has slowed down since the beginning of the 21st century [12].

In order to investigate the driving forces affecting vegetation cover, both natural circumstances and human activities should be taken into account. Climate change is one of the main driving forces of regional vegetation change [13]. By studying the effect of temperature change in spring on vegetation growth in North America [14,15] and the effect of a spring climate on the rate of vegetation greening in China [16], it was determined

that the increase in the NDVI is positively correlated with the increase in temperature. The vegetation growth is susceptible to precipitation. The evaporation in arid regions of the Southern Hemisphere is significant, and the correlation between the NDVI and precipitation is even higher. It has been found that precipitation decrease mainly causes a reduction in the NDVI [17]. As one of the essential non-zonal factors, the terrain factor is a vital shaping force of vegetation patterns. Riihimaki et al. [18] showed that altitude is the most crucial driving force affecting the NDVI in northwest Finland. In addition, the average NDVI during the growing season of the Taihang Mountain showed a single-peak curve distribution that increased at first and then decreased, while the altitude rose [19]. Meanwhile, with the rapid development of the social economy and the deepening of the role of human activities in the ecological environment, vegetation growth will also be inhibited or promoted [20]. The improvement of agricultural production levels and the implementation of ecological construction projects are important for the increase in the NDVI in northwest China [21]. Human activities such as construction encroachment on forest land, unreasonable farming methods, and the over-exploitation of water and hydrocarbon resources will negatively affect regional vegetation [9,22].

Despite several breakthroughs, there are still limitations in the study of the NDVI and its driving forces. Indeed, most current studies only focus on the impact of natural factors on the NDVI [23,24], e.g., studying and predicting the NDVI response to climate change in arid regions [25,26] or the relationship between vegetation growth and surface temperature in high latitudes of the Northern Hemisphere [27], while not considering human factors. The research objects focus on large-scale regions, such as the global scale [28,29], the Northern Hemisphere [30], and the high-latitude regions [31]. The research on NDVI in China is mainly concentrated on the Tibetan Plateau [32], the Yangtze River Basin [33], the Yellow River Basin [34] and other large areas. There is a lack of NDVI-related research on the small watersheds scale, especially in the Minjiang River Basin.

This study takes the Minjiang River, a tributary of the Yangtze River, as the research object. As an essential ecological barrier in the upper reaches of the Yangtze River, the Minjiang River Basin has a valuable strategic position for the protection of water resources. It is affected by topography and human activities, and the ecological environment is relatively fragile. Hence, under the impact of topography, climate and human activities, it is particularly important and necessary to recognize the characteristics of NDVI change in the Minjiang River Basin in China and to separate and quantify the relative contribution of different driving forces that affect vegetation change. The results help to deepen the understanding of the process of vegetation change in small watersheds, and provide scientific support for the protection of the ecological environment of the basin and the promotion of the green development of the local economy.

The contribution of different driving forces to vegetation change in the Minjiang River Basin in China is not clear. In the past, the analysis of the driving forces of vegetation change was mostly carried out through qualitative research, lacking the investigation of vegetation cover change and the analysis of future change trends. This study combines the Theil–Sen slope test, Mann–Kendall significance test, Rescaled Range Analysis and correlation analysis. It has high computational efficiency and a strong ability to avoid errors [35]. It can assess the spatial and temporal changes in the NDVI and effectively predict the trend of NDVI change in the region. In this study, through the Theil–Sen slope test and Mann–Kendall significance test, the temporal and spatial changes in the NDVI in the growing season in the Minjiang River Basin in China from 2001 to 2020 are discussed. Meanwhile, the future trend of the NDVI in the Minjiang River Basin is predicted using the Rescaled Range Analysis. Furthermore, the relationship between vegetation, topography, climate and human activities is revealed through a correlation analysis, which provides a scientific basis and theoretical reference for ecological environmental protection and vegetation restoration in the Minjiang River Basin.

2. Materials and Methods

2.1. Study Area

The Minjiang River Basin is located between latitudes 28°20′ N and 33°38′ N and longitudes 99°42′ E and 104°40′ E. It spans the Qinghai and Sichuan provinces in China (Figure 1). The basin includes the Guoluo Tibetan Autonomous Prefecture of Qinghai Province, Aba Tibetan and Qiang Autonomous Prefecture, Ganzi Tibetan Autonomous Prefecture, Chengdu, Ya'an, Meishan, Leshan, Liangshan Yi Autonomous Prefecture, Zigong and Yibin of Sichuan Province. It is one of the important tributaries in the upper reaches of the Yangtze River, with a drainage area of 136,000 km^2. The main stream of the Minjiang River originates from the southern foot of Minshan Mountain and flows into the main stream of the Yangtze River in Yibin from north to south [36], with a length of 711 km. The largest tributary of the Minjiang River is the Dadu River, with a total distance of 1062 km. It joins the Minjiang River in Leshan, with a drainage area of 77,700 km^2. The Qingyi River is a tributary of the Dadu River, and its primary source is the Baoxing River, with a length of 276 km and a drainage area of 13,300 km^2. The landforms of the Minjiang River Basin are complex and diverse, with the Zoige Plateau in the north, the Hengduan Mountain region in the west [37], the Yunnan-Guizhou Plateau in the south, and the Chengdu Plain in the east. The terrain gradually decreases from northwest to southeast. The highest altitude of the basin is 5568 m, the lowest altitude is 256 m, and the average altitude is 2912 m. The temperature and precipitation increase along with the terrain from north to south, and precipitation shows noticeable seasonal differences from June to September.
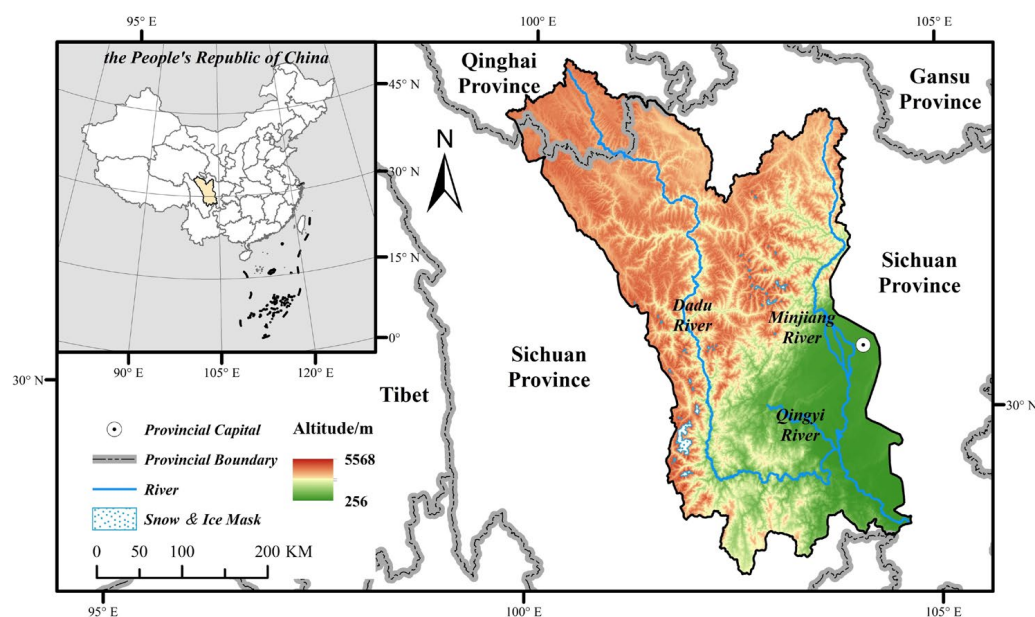
Figure 1. Location map of the Minjiang River Basin.

2.2. Data and Processing

2.2.1. NDVI Data

NDVI data are from the MOD13A1 data product with a spatial resolution of 500 m and a time resolution of 16 days from 2001 to 2020. It is published by the National Aeronautics and Space Administration (NASA). The orbit numbers are h25v05, h25v06, h26v05, and h26v06. The MODIS Reprojection Tool (MRT) was used to preprocess the MOD13A1 data [38,39], including format conversion and reprojection. The internationally accepted maximum value synthesis (MVC) method was used to maximize the NDVI data of each scene [40]. Finally, NDVI data were obtained for seven images in the growing season (April–October) of the Minjiang River Basin.

2.2.2. Climate Data and Nighttime Light Data

Meteorological and nighttime light data are from the National Tibetan Plateau Science data center (http://data.tpdc.ac.cn/zh-hans/, accessed on 20 April 2022) with a spatial resolution of about 1 km. Meteorological data include the average temperature and precipitation in the growing season (April–October) [41,42]. The data set is based on the global 0.5° climate data set released by the Climatic Research Unit (CRU) and the global high-resolution climate data set released by WorldClim [43]. A Delta spatial downscaling scheme is used to downscale the region in China, and the data of 496 independent meteorological observation points have been verified [44]. The nighttime light data are generated by the night light convolution long short-term memory (NTLSTM) network applied to the first set of the China Nighttime Light Dataset (PANDA) from 1984 to 2020. The data quality of the product is high, and the correlation between socio-economic indicators (built-up area, GDP, and population) and PANDA is better than all other existing products.

2.3. Methods

2.3.1. Theil–Sen Slope Test and Mann–Kendall Significance Test

The Theil–Sen (TS) slope test was used to estimate and analyze the variation trend of the NDVI in the Minjiang River Basin during the growing season in the period from 2001 to 2020 [45–48]. In addition, the Mann–Kendall (MK) significance test method was used to determine the significance of the variation trend [46,49,50]. The combination of the two methods can reduce the influence of abnormal values [51]. The Theil–Sen slope test takes the median of the slope as the overall trend of the time series change by calculating the slope between two data pairs in the time series [52]—Equation (1).

$$\text{Slope} = \text{Median}\left(\frac{\text{NDVI}_j - \text{NDVI}_i}{j - i}\right), \forall j > i \tag{1}$$

where Slope is the median of the slope of all data pairs. When Slope > 0, the vegetation change shows an upward trend, and when Slope < 0, the vegetation change shows a downward trend. NDVI_i and NDVI_j are the values of the years i and j in the NDVI time series, and Median is the median value.

To supplement the Theil–Sen slope test, the Mann–Kendall significance test is used to test the dominance of time series trends [53]—Equations (2)–(5).

$$Z = \begin{cases} \frac{S - 1}{\sqrt{\text{var}(S)}}, S > 0 \\ 0, S = 0 \\ \frac{S + 1}{\sqrt{\text{var}(S)}}, S < 0 \end{cases} \tag{2}$$

Among:

$$S = \sum_{i=1}^{n-1} \sum_{j=i+1}^{n} \text{sign}(\text{NDVI}_j - \text{NDVI}_i) \tag{3}$$

$$\text{var}(S) = \frac{n(n+1)(2n+5)}{18} \tag{4}$$

$$\text{sign}(\text{NDVI}_j - \text{NDVI}_i) = \begin{cases} 1, \text{NDVI}_j - \text{NDVI}_i > 0 \\ 0, \text{NDVI}_j - \text{NDVI}_i = 0 \\ -1, \text{NDVI}_j - \text{NDVI}_i < 0 \end{cases} \tag{5}$$

where n is the length of the data set, sign is the symbolic function, and NDVI_i and NDVI_j are the sets of sample time series data. When the absolute value of Z is greater than 1.96, the trend of the time series is significant at the given level of 0.05.

2.3.2. Hurst Index

The Hurst index can effectively predict the future change trend of time series [54], which is based on the Rescaled Range (R/S) analysis to simulate the sustainability of future changes in the NDVI of vegetation in the Minjiang River Basin—Equations (6)–(9).

Considering the time series {NDVI (i)}, where i = 1,2 . . . , n, for any positive integer m, the mean sequence is defined by Equation (6).

$$NDVI_m = \frac{1}{m}\sum_{i=1}^{m}NDVI_i, \ m = 1, 2, \cdots, n \tag{6}$$

Cumulative deviation:

$$X(t) = \sum_{i=1}^{m}(NDVI_i - NDVI_m), \ 1 \le t \le m \tag{7}$$

Range:

$$R(m) = \max_{1 \le t \le \tau} X(t) - \min_{1 \le t \le \tau} X(t), \ m = 1, 2, \cdots, n \tag{8}$$

Standard deviation:

$$S(m) = \sqrt{\frac{1}{m}\sum_{i=1}^{m}(NDVI_i - NDVI_m)^2}, \ m = 1, 2, \cdots, n \tag{9}$$

Considering the ratio R (m)/S (m)$\triangleq$R/S, if there is R/S $\propto$ m^H, it indicates that the time series {NDVI (i)}, i = 1, 2, . . . , n has the Hurst phenomenon, and H is called the Hurst index. According to the calculated value of (m, R/S), the H value can be obtained using the least square fitting formula in the double logarithmic coordinate system ln m, ln R/S.

The value of H = 0.5 indicates that the time series has a random sequence with random walk characteristics, i.e., no long-term correlation exists. If 0.5 < H < 1, it indicates that the time series has a persistent sequence with long-term correlation characteristics with stronger persistence closer to 1. If 0 < H < 0.5, it indicates that the time series data have anti-persistence, i.e., past variables are negatively correlated with future increment. In addition, the sequence has a sudden jump reversal and the closer it is to 0, the stronger the anti-persistence.

2.3.3. Correlation Analysis

A correlation analysis is mainly used to reflect the degree and direction of correlation between factors [9,55]. In this study, the correlation analysis based on pixels is mainly used. The correlation coefficient expresses the correlation between NDVI, temperature, precipitation, and nighttime light index. In the study, one element was fixed on the basis of the simple correlation coefficient, the partial correlation coefficient between the other two elements was calculated, and the correlation between the two elements was explored [56]—Equations (10) and (11).

$$R_{xy} = \frac{\sum_{i=1}^{n}[(x_i - \bar{x})(y_i - \bar{y})]}{\sqrt{\sum_{i=1}^{n}(x_i - \bar{x})^2}\sqrt{\sum_{i=1}^{n}(y_i - \bar{y})^2}} \tag{10}$$

where $\bar{x}$ and $\bar{y}$ are the average values of the two variables over n years, R_{xy} is the simple correlation coefficient between the two factors, and n is the sample.

$$R_{xy,z} = \frac{R_{xy} - R_{xz}R_{yz}}{\sqrt{(1 - R_{xz})^2}\sqrt{(1 - R_{yz})^2}} \tag{11}$$

where $R_{xy,z}$ are the partial correlation coefficients of the dependent variable x and the independent variable y after the fixed independent variable z.

3. Results

3.1. Temporal Variation of Vegetation

The interannual variation trend of the average NDVI in the growing season of the Minjiang River Basin from 2001 to 2020 was analyzed based on the linear regression analysis method (Figure 2). The results show that the average NDVI value in the growing season is between 0.56 and 0.64 with an average value of 0.60. The minimum value appeared in 2012, which may be the reason that the precipitation in the Minjiang River Basin is abundant, and the water required for vegetation growth is relatively sufficient. The rainfall in the growing season increased from 728.51 mm in 2011 to 900.95 mm in 2012. The sudden increase in rainfall led to increased cloud cover and reduced light, which reduced vegetation photosynthesis [57]. Meanwhile, the average temperature in the growing season decreased, which also negatively affected vegetation growth [58]. The maximum value of NDVI appeared in 2016. In the past twenty years, the NDVI in the Minjiang River Basin increased significantly with a rate of 0.002/a, showing a fluctuating growth trend.
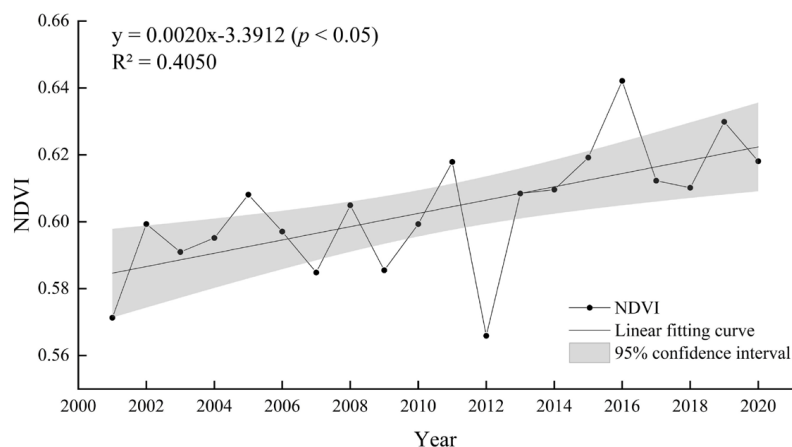

Figure 2. Interannual variation of NDVI in the growing season of the Minjiang River Basin from 2001 to 2020.

To better study the temporal variation of NDVI in the Minjiang River Basin, the NDVI values in 2001 and 2020 were divided into five classes (Table 1) [49,59]. Compared with 2001 (Figure 3a), the NDVI in the growing season in the Minjiang River Basin in 2020 (Figure 3b) increased, and the area with NDVI > 0.6 increased significantly. Moreover, the area with NDVI values between 0.6 and 0.8 increased the most, reaching a change in area of 21,904.41 km², indicating that the vegetation coverage has improved significantly.

Table 1. Changes in area and proportion of NDVI at all levels from 2001 to 2020.

| NDVI	2001		2020		2001–2020
	Area/km²	Percentage/%	Area/km²	Percentage/%	Area Change/km²
0–0.2	3458.47	2.56	2407.00	1.78	−1051.47
0.2–0.4	11,839.29	8.75	9812.49	7.25	−2026.80
0.4–0.6	59,120.57	43.69	36,318.21	16.84	−22,802.36
0.6–0.8	58,951.07	43.56	80,855.48	59.75	21,904.41
0.8–1	1957.65	1.45	5933.88	4.38	3976.22
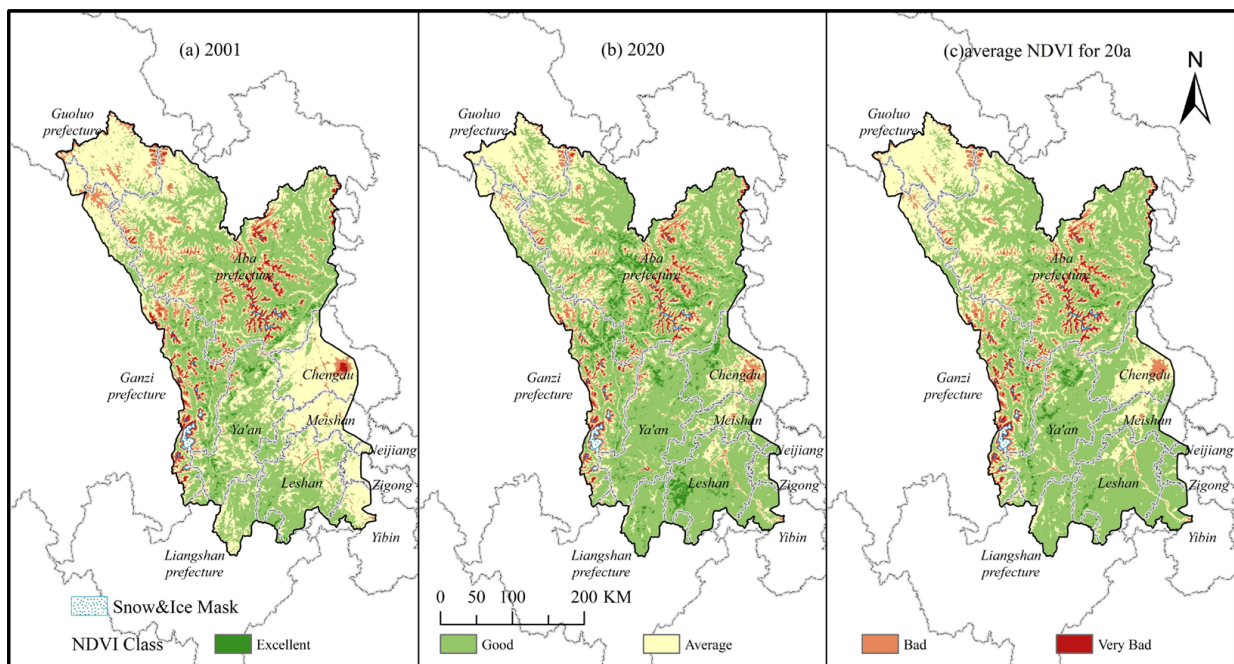
Figure 3. Spatial distribution of NDVI in Minjiang River Basin during the growing season.

3.2. Spatial Distribution Characteristics of Vegetation Evolution

According to the spatial distribution of the average NDVI values in the Minjiang River Basin during the growing season in the last 20 years (Figure 3c), the areas with good vegetation growth in the basin are mainly located in Ya'an and western Leshan.

According to the pixel-by-pixel Theil–Sen slope test (Figure 4a) and Mann–Kendall significance test (Figure 4b) of the NDVI in the growing season in the Minjiang River Basin, the area passing the MK test ($p < 0.05$) is 96,237.12 km^2. It accounts for 71.11% of the basin area, and the overall trend is relatively obvious. Combined with the TS slope and the MK test (Figure 4c), the slope estimation results were divided into five classes (Table 2) [60].
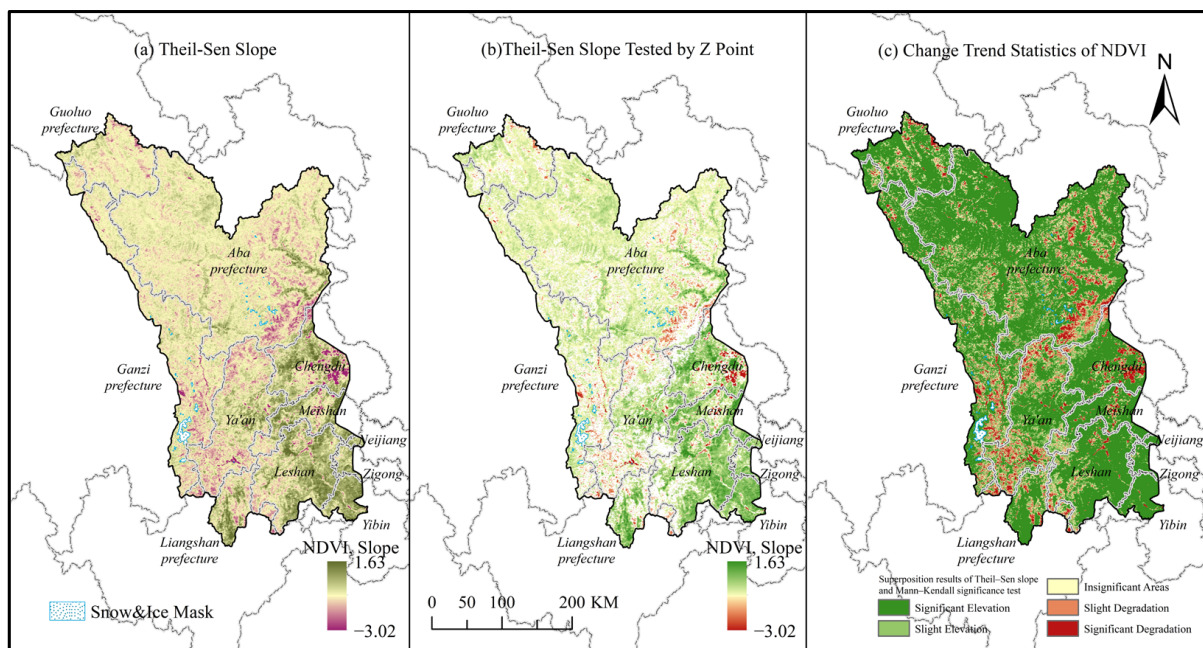
Figure 4. Spatial distribution of Theil–Sen slope of average NDVI in the growing season in the Minjiang River Basin from 2001 to 2020 and the superposition result with Mann–Kendall test.

Table 2. Classification table of NDVI change trend from 2001 to 2020.

Slope $_{NDVI}$	Z	NDVI Change Trend	Area/km^2	Area Percentage/%
≥0.0005	|Z| > 1.96	Significant improvement	89,340.90	66.02
≥0.0005	−1.96 ≤ Z ≤ 1.96	Slight improvement	17,576.95	12.99
0.0005~0.0005	-	Stable and unchanging	14,354.64	10.61
≤−0.0005	−1.96 ≤ Z ≤ 1.96	Slight degradation	7335.84	5.42
≤−0.0005	|Z| > 1.96	Significant degradation	6718.73	4.96

The NDVI change trend of the basin in the past twenty years was dominated by an obvious improvement, with an area of 89,340.90 km^2. It accounts for 66.02% of the total area of the basin. It was mainly distributed in the southeast, central and northern low-altitude areas of the basin, such as the central urban area of Chengdu, western Chengdu, Leshan, and central Meishan. The significantly degraded area is 6718.73 km^2, accounting for 4.96% of the basin area. It is mainly distributed in areas with rapid urban expansion and rapidly rising altitude, such as southern Chengdu, southern and northern Ya'an, and southern Aba Prefecture.

3.3. Sustainability Analysis of Vegetation Evolution

The average Hurst index of the NDVI in the Minjiang River Basin growing season is 0.43, and it is mainly anti-persistent (Figure 5a). The area with a Hurst index of more than 0.5 is 26,956.87 km^2, accounting for 19.92% of the basin area and showing persistence. The future NDVI trend is the same as in the past, mainly distributed in the north of Chengdu. Otherwise, the area with a Hurst index of less than 0.5 is 108,370.19 km^2, accounting for 80.08% of the basin area, which shows anti-sustainability. The trend of the NDVI in the future is opposite to that in the past.
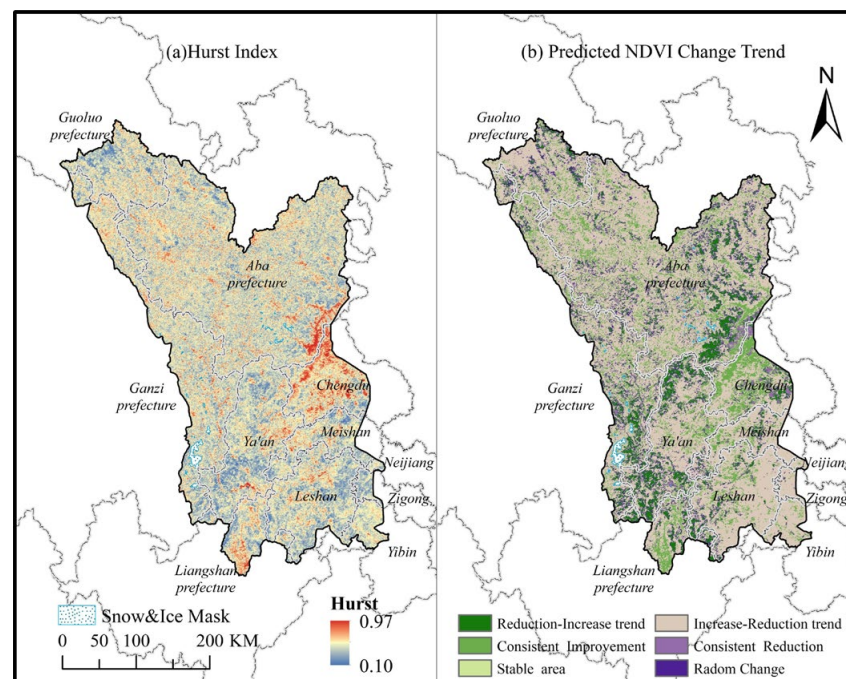
Figure 5. Hurst index of average NDVI and spatial distribution map of change sustainability in the Minjiang River Basin.

Combining the Hurst index with the Theil–Sen slope (Figure 5b) [61], the future trend of NDVI in the Minjiang River Basin was predicted (Table 3). The results show that the area from degradation to improvement is 10,883.25 km^2, which accounts for 8.04% and is mainly distributed in the south of Ya'an, east of Ganzi Prefecture and south of Aba

Prefecture. The area of continuous improvement is 21,361.58 km^2, accounting for 15.79% and is mainly distributed in Chengdu. The area of the region that remains unchanged is 2424.55 km^2, accounting for 1.79%, with a small distribution. The area from improvement to degradation is 85,556.67 km^2, accounting for 63.22% and is widely distributed throughout the basin. The area of continuous degradation is 3170.74 km^2, accounting for 2.34%, and is mainly distributed in the south of Aba Prefecture and around the built-up area of Chengdu downtown. It shows that along with the expansion of the city, areas with high vegetation coverage around the built-up area may be transformed into urban land, decreasing the NDVI. The area of future random variation is 11,930.26 km^2, accounting for 8.82%, and is mainly distributed in the boundary between the two anti-persistent distribution areas of improvement to degradation and degradation to improvement. Overall, the area from improvement to degradation was the largest, accounting for 63.22%, which indicates a risk of future degradation of the vegetation cover in the Minjiang River Basin. Future development should pay attention to the protection of the ecological environment.

Table 3. Classification table of NDVI change persistence.

Slope $_{NDVI}$	Hurst Index	Persistence of Changes in NDVI	Area/km^2	Area Ratio/%
≤ -0.0005	0~0.5	From degradation to improvement	10,883.25	8.04
≥ 0.0005	0.5~1	Continuous improvement	21,361.58	15.79
-0.0005~0.0005	0.5~1	Persistent	2424.55	1.79
≥ 0.0005	0~0.5	From improvement to degradation	85,556.67	63.22
≤ -0.0005	0.5~1	Continuous degradation	3170.74	2.34
-0.0005~0.0005	0~0.5	Random variation	11,930.26	8.82

*3.4. NDVI Driving Force Analysis*

3.4.1. Spatial-Temporal Variation Characteristics of Climate and Human Activities

The interannual variation trends of average temperature, accumulated precipitation, and nighttime light index in the growing season in the Minjiang River Basin from 2001 to 2020 were analyzed using the linear regression method (Figure 6). In the past 20 years, the average temperature in the growing season in the basin (Figure 6a) was 11.09 °C, which increased at a rate of 0.016 °C/a. The average accumulated precipitation in the growing season in the last 20 years (Figure 6b) was 834.17 mm, which increased at a rate of 6.764 mm/a. The average nighttime light in the past 20 years (Figure 6c) increased at a rate of 0.051/a. With a significant increase in the urbanization rate [62], the nighttime light index increased from 0.81 in 2001 to 1.88 in 2020, with a growth rate of 132%.

The pixel-by-pixel slope estimation of the average temperature, cumulative precipitation, and nighttime light index in the growing season in the Minjiang River Basin was conducted to obtain the spatial variation trend of the three factors (Figure 7). The temperature in the eastern plains of the basin had an upward trend (Figure 7a), while the temperature changes in the western and northern mountainous areas were significantly influenced by the slope direction. The overall trend indicated that the temperature in the western and southern slopes increased, and the temperature in the eastern and northern slopes decreased. In addition, there are significant differences in the rate of temperature change in different slope aspects. The temperature growth rate on the west slope (247.5°–292.5°) is the fastest and reaches 0.033 °C/a, and the temperature decline rate on the east slope (67.5°–112.5°) is 0.001 °C/a (Table 4). The variation trend of accumulated precipitation during the growing season (Figure 7b) was greatly affected by altitude and topographic relief, and the overall trend decreased from southeast to northwest. Precipitation in the low-altitude area of the southeast has increased significantly. The increasing precipitation trend in the low-altitude plains and mid-relief mountains in the central topographic transition zone gradually decreased. Precipitation decreased in the mountainous and alpine regions in the undulating western areas. Figure 7c shows the significant urban expansion of Chengdu, which has increased the nighttime light index around the central

urban area. In addition, the nighttime light index of cities with rapid economic growth, such as Meishan and Leshan, also increased significantly.
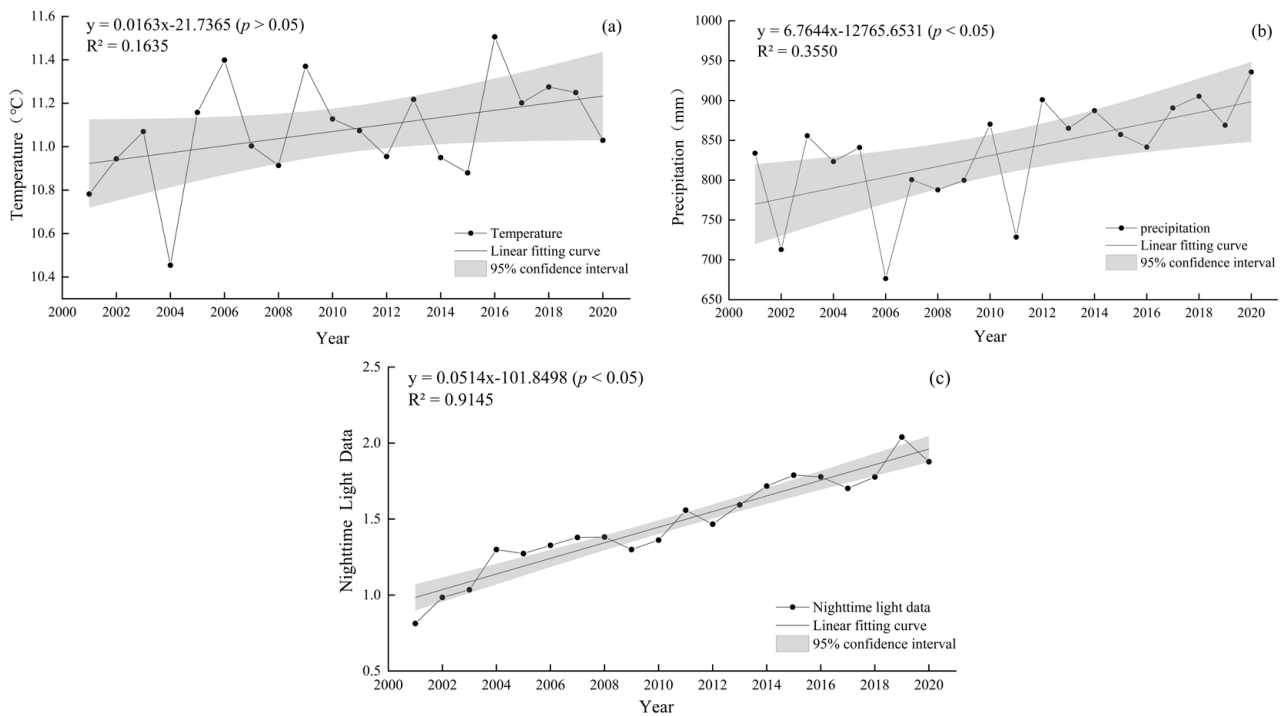
Figure 6. Annual variation trend of temperature (**a**), precipitation (**b**) and nighttime light index (**c**) in the Minjiang River Basin from 2001 to 2020.
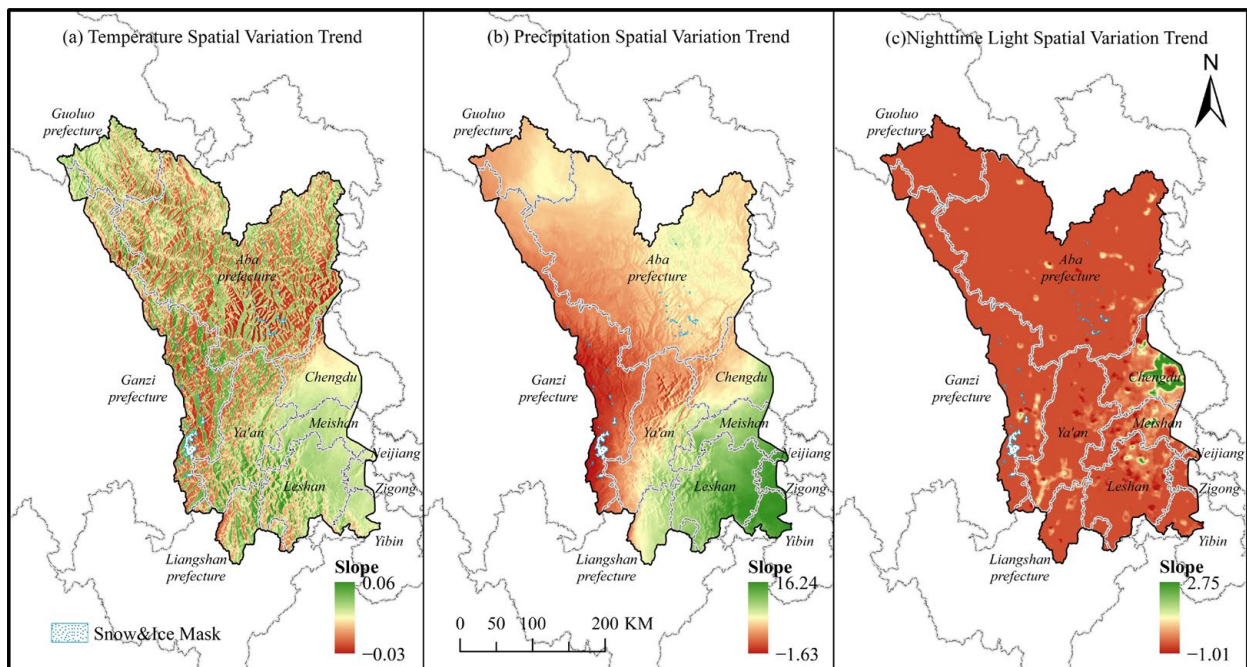

Figure 7. Trends of average temperature, accumulated precipitation and nighttime light during the growing season in the Minjiang River Basin from 2001 to 2020.

Table 4. Temperature variation trend in the Minjiang River Basin based on different slope directions from 2001 to 2020.

Aspect	Plane	North	Northeast	East	Southeast	South	Southwest	West	Northwest
Slope × 100	1.89	1.69	0.42	0.05	0.21	1.36	2.83	3.33	2.97

3.4.2. Correlation Analysis between NDVI and Topographic Factors

By extracting the NDVI values of the growing season in the Minjiang River Basin from 2001 to 2020 at different altitudes (Figure 8), the changes in the NDVI with altitude were divided into five stages. At altitudes of 256–383 m, the NDVI increased rapidly with the increase in altitude. At altitudes of 383–496 m, the NDVI decreased with increased construction land. At altitudes of 496–588 m, the NDVI increased significantly with altitude. As the altitude gradually increases into the mountains, the vegetation coverage increases significantly. At altitudes of 588–3471 m, there was no significant change in the NDVI. The altitude range was from the valley to the transition zone of middle and high mountains and alpine canyons [63]. Vegetation types were complex and diverse, and vegetation coverage was high. Therefore, the NDVI was relatively stable. At altitudes of 3471–5568 m, the NDVI decreased significantly with the increase in altitude due to extreme climatic conditions in the alpine regions that limited the growth and development of vegetation.
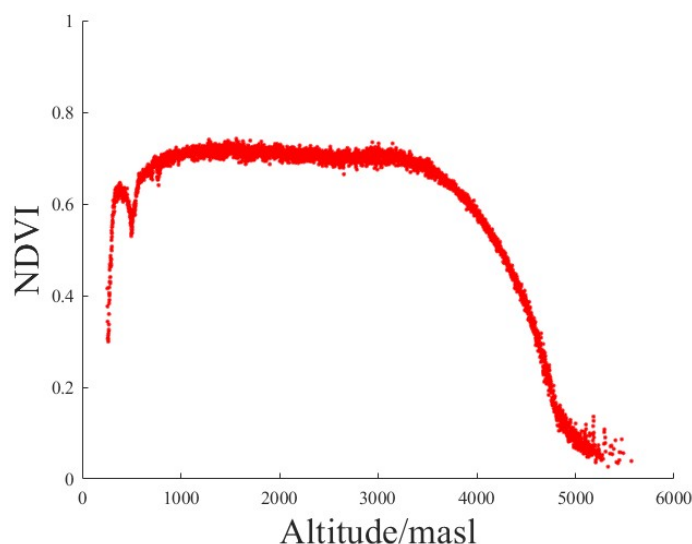
Figure 8. Relationship between NDVI and altitude in the growing season in the Minjiang River Basin from 2001 to 2020.

By extracting the average value of the NDVI in the Minjiang River Basin during the growing season under different slope grades (Figure 9), the average value of the NDVI in the basin is divided into four stages. The average NDVI on slopes between 0° and 5° was higher than that on slopes 5°–10°, which is mainly related to the relatively high level of greening in the eastern plain. On slopes 5°–25°, the average NDVI gradually increased with the slope. At this stage, with the slope increase, human activities gradually decreased, which was conducive to vegetation growth and development. On slopes 25°–40°, the growth rate of the NDVI slowed down, and vegetation cover was good, with less human activities and less impact on the region, and the NDVI was relatively stable. When the slope was 40°–45°, the NDVI began to decline. Finally, when the slope was greater than 45°, the average NDVI decreased sharply because the slope was too large and the terrain was steep, which was not suitable for vegetation growth.
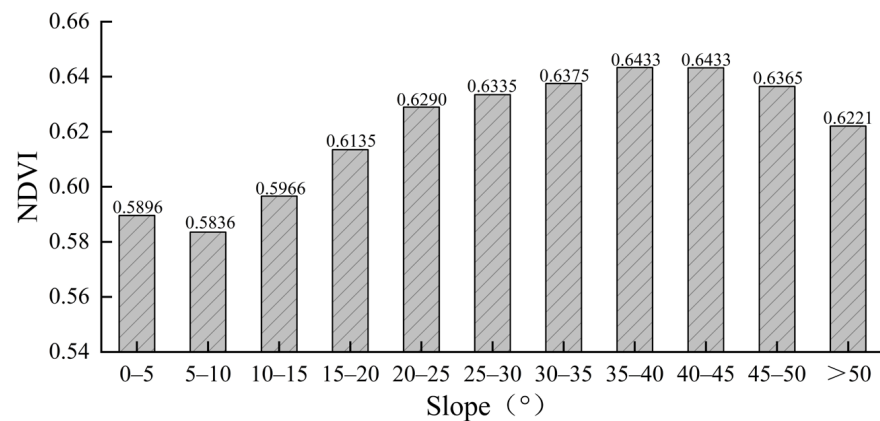
Figure 9. Relationship between average NDVI and slope in the growing season in the Minjiang River Basin from 2001 to 2020.

3.4.3. Partial Correlation Analysis of NDVI with Climate and Human Activities

The results of the partial correlation analysis (Figure 10) show that the correlation between climate factors and NDVI changes in the Minjiang River Basin is more obvious than human activities, which is the main reason for vegetation improvement and is the same as the study of Xu et al. [64]. The average values of partial correlation coefficients between the NDVI and temperature, precipitation, and nighttime light index were 0.46, 0.31 and 0.27, respectively. The regions that passed the significance test ($p < 0.05$) were all dominated by a significant positive correlation. The area of significant correlation between the NDVI and temperature was 13,308.66 km^2 (Figure 10a), and the area of significant positive correlation was 9.02% of the basin area. It was mainly distributed in small undulating low mountains and low-altitude hilly areas, such as eastern Ya'an, western Meishan and Leshan. The area of significant correlation between the NDVI and precipitation was 20,651.73 km^2 (Figure 10b), and the area of significant positive correlation was 11.59% of the basin area. It was mainly distributed in the lower altitude areas of the southeast and north of the basin, such as eastern Leshan, northwestern Yibin, the lower altitude area in Aba Prefecture and Banma County, Qinghai Province. The area of significant correlation between the NDVI and nighttime light index was 13,134.66 km^2 (Figure 10c), and the area of significant positive correlation was 7.16% of the basin area. It was mainly distributed in the peripheral counties of Chengdu and areas with human activities along the Qingyi River, such as northwestern Chengdu, eastern Ya'an, and northern Leshan.

3.4.4. NDVI Response to Different Driving Factors

The NDVI showed an increasing trend at first and then decreased with the increase in altitude and slope, with 3471 m and 40° as the boundaries. There were also noticeable periodic changes. In the west and north of Minjiang River Basin, with the increase in altitude, the slope gradient was not conducive for soil and water conservation, resulting in a decrease in the NDVI. At the same time, the adaptability of vegetation in the region was poor, and it was vulnerable to disturbance and degradation [65].

Climate change mainly promotes vegetation growth in the basin, and the influence of temperature on NDVI is greater than that of precipitation [66]. Plains and terraces with low altitude and small fluctuation in the southeast of the basin showed a relative trend of damp-heat. It benefits vegetation growth and promotes vegetation improvement and restoration. The partial correlation coefficient between the NDVI and precipitation in the western part of the basin showed an obvious spatial differentiation. There was a significant positive correlation in low-altitude valley areas and a significant negative correlation in high-altitude areas, indicating that altitude greatly affects vegetation growth in the Minjiang River Basin [64].
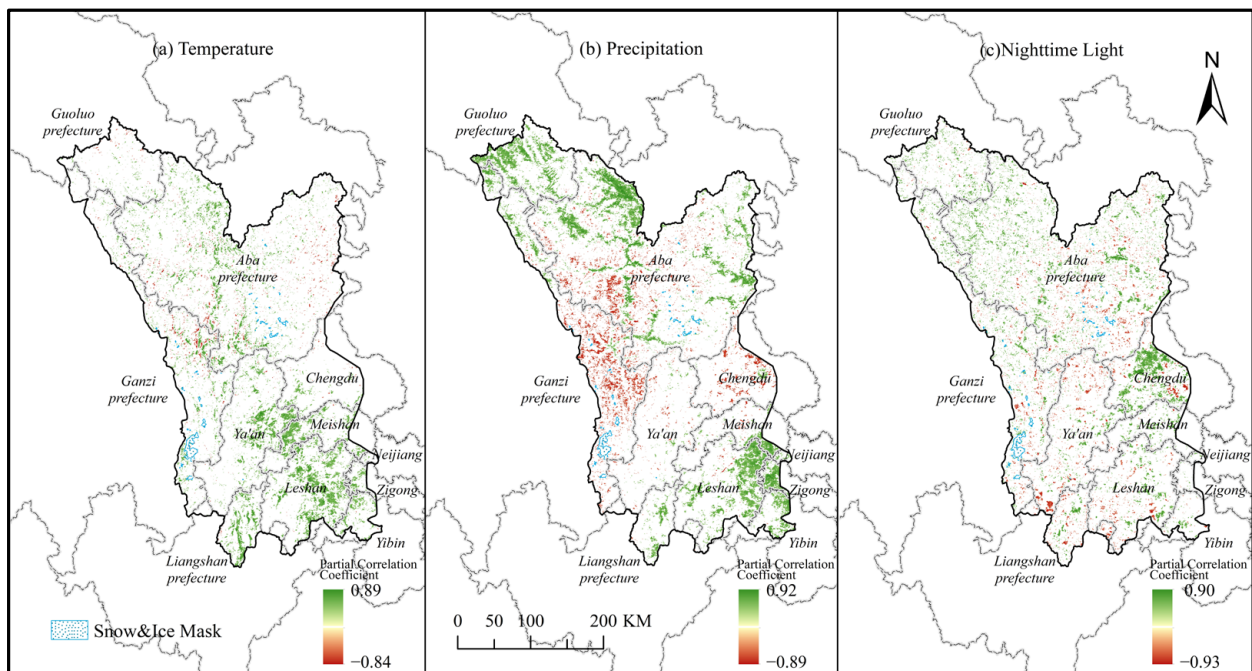
Figure 10. Partial correlation coefficient between NDVI and temperature, precipitation and nighttime light in the growing season in the Minjiang River Basin from 2001 to 2020.

Human activities have shown duality in the growth of vegetation in the basin. The NDVI was positively correlated with the nighttime light index in some areas. The nighttime light index has increased significantly, which indicates that with urban expansion, more attention is being paid to protecting the ecological environment and several measures are being taken to improve the vegetation cover. In some areas of rapid economic development, strong human disturbance, population growth, unreasonable land use and other reasons [67] can decrease the level of vegetation cover. However, the NDVI in the growing season in the Minjiang River Basin has showed an upward trend in the past 20 years, indicating that the decline in the NDVI in some areas did not change the greening trend of the whole region during the urban expansion process, which is consistent with the results of Chen et al. [68].

4. Discussion

4.1. Spatial-Temporal Evolution Characteristics of Vegetation

The average NDVI in the Minjiang River Basin during the growing season from 2001 to 2020 was 0.60 and increased at a rate of 0.002/a. This result is consistent with the study of Sun [69] about the Minjiang River Basin. In 2012 and 2016, NDVI values fluctuated greatly, indicating that the NDVI was susceptible to climate or human activities. The average growth rate of the NDVI obtained in this study is lower than in previous studies because the monthly NDVI was composited by the MVC method, and the annual NDVI was composited by the average NDVI from April to October. When the annual NDVI is composited by the MVC method, the calculated annual maximum NDVI is higher than that measured or estimated by other remote sensing estimation methods [70]. From the perspective of spatial distribution, the areas with significantly improved vegetation in the basin are mainly distributed in the southeast and the lower altitude in the central and northern parts of the basin, such as the center of Chengdu, Leshan, and northern Yibin. Currently, research on the NDVI in the Minjiang River Basin is only concentrated on the upper reaches of the Minjiang River [71,72], and there is little research on the NDVI in the whole Minjiang River Basin. According to the research on NDVI spatial-temporal changes in the Yangtze River Basin [33,73] and Qinghai-Tibet Plateau [74], the spatial evolution

characteristics of the NDVI in the growing season in the Minjiang River Basin in the past 20 years are consistent with those of previous studies.

4.2. Effects of Different Driving Factors on Spatial-Temporal Evolution of Vegetation

Climate change mainly promotes vegetation growth in the Minjiang River Basin, which is consistent with research by Hou et al. [75] in the Southwestern Karst Region of China and research by Wen et al. [76] in the Three Gorges Reservoir Region, China. Climate warming prolonged the growth cycle of vegetation in the Minjiang River Basin [77]. It accelerated the decomposition of soil organic matter and the release of nutrient elements [78], which is beneficial to the accelerated growth of vegetation. The vegetation improvement in the southeastern plains and northern mountainous areas of the basin is due to the damp-heat trend. On the other hand, climate factors can also inhibit vegetation growth. Zhang et al. [79] noted that when the temperature increase exceeds the optimal value required for vegetation growth, the growth of vegetation will be seriously hindered due to increased evaporation. Low temperatures can lead to insufficient accumulated temperature and reduce plant photosynthesis, affecting plant growth [80]. In high altitude areas with large topographic relief, the large altitude difference can lead to low pressure, limiting the growth of grass vegetation [81]. The low NDVI in the high-altitude areas of the Minjiang River Basin is due to extreme low-temperature conditions.

In addition to climatic factors, human activities are also an important driving factor affecting vegetation cover changes. Human activities such as improving agricultural management and implementing vegetation construction projects can effectively increase vegetation coverage in local areas and at regional scales [8]. Jiang et al. [54] noted that land use and land cover changes due to human activities are one of the main reasons for the changes in the NDVI. Zhang et al. [82] noted that human activities play an important role in vegetation restoration after the 21st century, and ecological protection and construction actions have achieved initial results. The project of returning farmland to forests, which was promoted in 2002, has rapidly expanded the forest area in Sichuan [83]. Moreover, the forest coverage rate, artificial forest area and total afforestation area in the Minjiang River Basin have increased annually [73]. In 2018, Chengdu city proposed the concept of Park City. In 2021, the forest coverage rate of Chengdu increased to 40.3%. The improvement of vegetation coverage in the central urban area of Chengdu benefits from the promulgation and implementation of several policies. On the other hand, the negative impact of human activities on vegetation change is particularly obvious in large cities and is mainly related to the encroachment of urbanization on farmland and woodland, which results in the decrease in vegetation cover in some areas [84]. Liu et al. [85] found that due to the conversion of a large number of farmlands to construction land in the Yangtze River Delta, the NDVI decreased. Vegetation degradation in the surrounding areas of the central urban area of Chengdu is due to urban expansion.

The spatial differentiation of the NDVI is mainly affected by topography and climatic factors in the Minjiang River Basin, and there is a significant interaction between these factors [64]. The sunshine duration in different slope directions and the thermal insulation effects of clouds are different [86], which affects the heat radiation and leads to significant differences in the rate of temperature growth. Altitude has a significant influence on precipitation changes. The precipitation growth rate in low-altitude plains and platforms is high, while the precipitation growth rate in high-altitude areas is low or negative.

4.3. Research Methods of Driving Factors of NDVI

Currently, driving factors research methods include correlation analysis, residual analysis, the geographic detector model and other methods. This study used the correlation method to obtain the average value of the NDVI at different altitudes and slopes. Meanwhile, the partial correlation coefficients between the average temperature of the growing season, cumulative precipitation, nighttime light index, and NDVI of the growing season in the Minjiang River Basin from 2001 to 2020 were calculated. The results clearly show

the influence of climate and human activities on the NDVI in the basin. This study did not use the multiple regression residual analysis [87] for the assessment of the impact of human activities on vegetation cover because there are some deficiencies in the application of this method to separate the impact of human activities on NDVI changes. For example, when establishing the multiple regression equation between climatic factors and the NDVI, there is no conclusion on how to select reasonable climatic factors [88]. When referring to human activities, it does not consider specific aspects such as the vegetation construction [89], change in forest and grassland by construction land [84], agricultural technology progress, and accelerated urbanization. In addition to climate and human activities, other factors such as soil moisture or type can also affect regional changes in the NDVI. Although the contribution of human activities to vegetation changes can be measured to a certain extent by a residual analysis, the impact of climate cannot be completely ruled out [90]. In recent years, the geographical detector model [91] has been applied to detect the spatial differentiation of the NDVI and discover its driving forces, which is conducive for refining the driving factors of vegetation change and determining the relationship between various factors and vegetation change.

5. Conclusions

Based on the long-time series of NDVI data from MODIS, this study analyzes the temporal and spatial evolution characteristics of the NDVI in the Minjiang River Basin from 2001 to 2020. It predicts the sustainability and evolution trend of the NDVI in the future, analyzes the relationship between the NDVI and altitude and slope, considers the partial correlation between the NDVI and temperature, precipitation and nighttime light, and explores the driving mechanism of NDVI spatial-temporal evolution in the Minjiang River Basin. The main conclusions are as follows:

(1) Vegetation growth in the Minjiang River Basin during the growing season was good, with an average NDVI of 0.60 and a growth rate of 0.002/a.

(2) The changing trend of the NDVI in the growing season in the Minjiang River Basin was relatively obvious. The area accounted for 71.11%, according to the MK test, which was dominated by a noticeable improvement, accounting for 66.02% of the basin area. The Hurst index shows that the future trend of the NDVI in the Minjiang River Basin is mainly anti-sustained, with 63.22% of the area expected to change from improvement to degradation, and 15.79% of the area continuing to improve.

(3) The average temperature in the growing season in the Minjiang River Basin increased at a rate of 0.016 °C/a from 2001 to 2020. Moreover, the cumulative precipitation increased significantly at a rate of 6.764 mm/a, and there was apparent spatial differentiation. Furthermore, average nighttime light increased at a rate of 0.051/a.

(4) The spatial differentiation of the NDVI in the Minjiang River Basin during the growing season was mainly affected by topography and climate, followed by human activities. The NDVI initially showed an increasing trend and then decreased with an increasing altitude and slope, with obvious periodic changes. The average partial correlation coefficients of the NDVI with temperature, precipitation, and nighttime light index were 0.46, 0.31, and 0.27, respectively. Climate change and human activities played a major role in promoting vegetation growth in the basin.

The quality of the NDVI data was not checked in this study. MOD13 is a 16-day composite vegetation index product, which is affected by noise such as cloud cover that can cause many outliers. MODIS data come with a quality control file, which can filter out only low-quality pixels. In the future, the Savitzky–Golay Filter (SG filter) can be considered to reduce or eliminate these outliers [92,93].

Previous studies have shown that meteorological factors, especially precipitation, have a significant hysteresis effect on the NDVI [94,95]. In the future, a sliding time series window analysis can be considered in order to investigate the hysteresis mechanism.

This study divides the change law of climate according to different terrains and combines the partial correlation between the NDVI and climatic factors to investigate the

driving mechanism of climate on the NDVI. It does not discuss in detail the correlation between terrain and climate change and their indirect impact on the NDVI. Many related studies have explained the driving mechanism of the NDVI from the perspective of other meteorological factors (wind speed, snow depth, and humidity) [96], land use change [97], atmospheric CO_2 concentration, and nitrogen deposition [98]. In the future, the geographical detector model can be used to consider the impact of multiple factors on the NDVI, such as sunshine hours, solar radiation, relative humidity, land use and land cover changes, population migration, GDP, vegetation net primary productivity (NPP), and vegetation type. At the same time, the geographical detector model can also analyze the interaction between different factors and more accurately investigate the influencing factors of the NDVI.

Abbreviations

$NDVI_i$	NDVI value in year i
$NDVI_m$	NDVI value of time series NDVI(i)
$Slope_{NDVI}$	Slope of NDVI change
Z	The test statistics of the Z test
H	Hurst index

References

1. Walther, G.R.; Post, E.; Convey, P.; Menzel, A.; Parmesank, C.; Beebee, T.J.C.; Fromentin, J.M.; Hoegh-GuldbergI, O.; Bairlein, F. Ecological responses to recent climate change. *Nature* **2002**, *416*, 389–395. [CrossRef] [PubMed]
2. Nemani, R.R.; Keeling, C.D.; Hashimoto, H.; Jolly, W.M.; Piper, S.C.; Tucker, C.J.; Myneni, R.B.; Running, S.W. Climate-driven increases in global terrestrial net primary production from 1982 to 1999. *Science* **2003**, *300*, 1560–1563. [CrossRef] [PubMed]
3. Dong, Y.; Yin, D.Q.; Li, X.; Huang, J.X.; Su, W.; Li, X.C.; Wang, H.S. Spatial–temporal evolution of vegetation NDVI in association with climatic, environmental and anthropogenic factors in the Loess Plateau, China during 2000–2015: Quantitative analysis based on geographical detector model. *Remote Sens.* **2021**, *13*, 4380. [CrossRef]
4. Huang, S.; Tang, L.N.; Hupy, J.P.; Wang, Y.; Shao, G.F. A commentary review on the use of normalized difference vegetation index (NDVI) in the era of popular remote sensing. *J. For. Res.* **2021**, *32*, 1–6. [CrossRef]
5. Leng, S.; Huete, A.; Cleverly, J.; Yu, Q.; Zhang, R.R.; Wang, Q.F. Spatiotemporal variations of dryland vegetation phenology revealed by satellite-observed fluorescence and greenness across the North Australian Tropical Transect. *Remote Sens.* **2022**, *14*, 2985. [CrossRef]
6. Leng, S.; Huete, A.; Cleverly, J.; Gao, S.C.; Yu, Q.; Meng, X.Y.; Qi, J.Y.; Zhang, R.R.; Wang, Q.F. Assessing the impact of extreme droughts on dryland vegetation by multi-satellite solar-induced chlorophyll fluorescence. *Remote Sens.* **2022**, *14*, 1581. [CrossRef]
7. Zeng, J.Y.; Zhang, R.R.; Qu, Y.P.; Bento, V.A.; Zhou, T.; Lin, Y.H.; Wu, X.P.; Qi, J.Y.; Shui, W.; Wang, Q.F. Improving the drought monitoring capability of VHI at the global scale via ensemble indices for various vegetation types from 2001 to 2018. *Weather Clim. Extreme.* **2022**, *35*, 100412. [CrossRef]

8. Xin, Z.B.; Xu, J.X.; Zheng, W. Spatiotemporal variations of vegetation cover on the Chinese Loess Plateau (1981–2006): Impacts of climate changes and human activities. *Sci. China Ser. D Earth Sci.* **2008**, *51*, 67–78. [CrossRef]

9. Chu, H.S.; Venevsky, S.; Wu, C.; Wang, M.H. NDVI-based vegetation dynamics and its response to climate changes at Amur-Heilongjiang River Basin from 1982 to 2015. *Sci. Total Environ.* **2019**, *650*, 2051–2062. [CrossRef]

10. Eastman, J.R.; Sangermano, F.; Machado, E.A.; Rogan, J.; Anyamba, A. Global trends in seasonality of normalized difference vegetation index (NDVI), 1982–2011. *Remote Sens.* **2013**, *5*, 4799–4818. [CrossRef]

11. Mohammat, A.; Wang, X.H.; Xu, X.T.; Peng, L.Q.; Yang, Y.; Zhang, X.P.; Myneni, R.B.; Piao, S.L. Drought and spring cooling induced recent decrease in vegetation growth in Inner Asia. *Agric. Forest Meteorol.* **2013**, *178–179*, 21–30. [CrossRef]

12. Peng, S.S.; Chen, A.P.; Xu, L.; Cao, C.X.; Fang, J.Y.; Myneni, R.B.; Pinzon, J.E.; Tucker, C.J.; Piao, S.L. Recent change of vegetation growth trend in China. *Environ. Res. Lett.* **2011**, *6*, 44027. [CrossRef]

13. Huang, X.L.; Zhang, T.B.; Yi, G.H.; He, D.; Zhou, X.B.; Li, J.J.; Bie, X.J.; Miao, J.Q. Dynamic changes of NDVI in the growing season of the Tibetan Plateau during the past 17 years and its response to climate change. *Int. J. Environ. Res. Public Health* **2019**, *16*, 3452. [CrossRef]

14. Wang, X.H.; Piao, S.L.; Ciais, P.; Li, J.S.; Friedlingstein, P.; Koven, C.; Chen, A.P. Spring temperature change and its implication in the change of vegetation growth in North America from 1982 to 2006. *Proc. Natl. Acad. Sci. USA* **2011**, *108*, 1240–1245. [CrossRef]

15. Zhang, R.R.; Qi, J.Y.; Leng, S.; Wang, Q.F. Long-term vegetation phenology changes and responses to preseason temperature and precipitation in Northern China. *Remote Sens.* **2022**, *14*, 1396. [CrossRef]

16. Cong, N.; Wang, T.; Nan, H.J.; Ma, Y.C.; Wang, X.H.; Myneni, R.B.; Piao, S.L. Changes in satellite-derived spring vegetation green-up date and its linkage to climate in China from 1982 to 2010: A multimethod analysis. *Glob. Change Biol.* **2013**, *19*, 881–891. [CrossRef]

17. Ichii, K.; Kawabata, A.; Yamaguchi, Y. Global correlation analysis for NDVI and climatic variables and NDVI trends: 1982–1990. *Int. J. Remote Sens.* **2002**, *23*, 3873–3878. [CrossRef]

18. Riihimäki, H.; Heiskanen, J.; Luoto, M. The effect of topography on arctic-alpine aboveground biomass and NDVI patterns. *Int. J. Appl. Earth Obs.* **2017**, *56*, 44–53. [CrossRef]

19. Hu, S.; Wang, F.Y.; Zhan, C.S.; Zhao, R.X.; Mo, X.G.; Liu, L.M.Z. Detecting and attributing vegetation changes in Taihang Mountain, China. *J. Mt. Sci.* **2019**, *16*, 337–350. [CrossRef]

20. Jiang, M.C.; Tian, S.F.; Zheng, Z.J.; Zhan, Q.; He, Y.X. Human activity influences on vegetation cover changes in Beijing, China, from 2000 to 2015. *Remote Sens.* **2017**, *9*, 271. [CrossRef]

21. Dai, S.P.; Zhang, B.; Wang, H.J.; Wang, Y.M.; Guo, L.X.; Wang, X.M.; Li, D. Vegetation cover change and the driving factors over northwest China. *J. Arid Land* **2011**, *3*, 25–33.

22. Meng, M.; Huang, N.; Wu, M.Q.; Pei, J.; Wang, J.; Niu, Z. Vegetation change in response to climate factors and human activities on the Mongolian Plateau. *PeerJ* **2019**, *7*, e7735. [CrossRef] [PubMed]

23. Liu, Y.; Lu, Y.H.; Zheng, H.F.; Chen, L.D. Application of regression tree in analyzing the effects of climate factors on NDVI in loess hilly area of Shaanxi Province. *Chin. J. Appl. Ecol.* **2010**, *21*, 1153–1158.

24. Shang, J.X.; Zhang, Y.; Peng, Y.; Huang, Y.H.; Zhu, L.; Wu, Z.Y.; Wang, J.; Cui, Y.X. Climate change drives NDVI variations at multiple spatiotemporal levels rather than human disturbance in Northwest China. *Environ. Sci. Pollut. Res.* **2022**, *29*, 13782–13796. [CrossRef]

25. Xu, Y.F.; Yang, J.; Chen, Y.N. NDVI-based vegetation responses to climate change in an arid area of China. *Theor. Appl. Climatol.* **2016**, *126*, 213–222. [CrossRef]

26. Martiny, N.; Philippon, N.; Richard, Y.; Camberlin, P.; Reason, C. Predictability of NDVI in semi-arid African regions. *Theor. Appl. Climatol.* **2010**, *100*, 467–484. [CrossRef]

27. Myneni, R.B.; Keeling, C.D.; Tucker, C.J.; Asrar, G.; Nemani, R.R. Increased plant growth in the northern high latitudes from 1981 to 1991. *Nature* **1997**, *386*, 698–702. [CrossRef]

28. Wu, D.H.; Zhao, X.; Liang, S.L.; Zhou, T.; Huang, K.C.; Tang, B.J.; Zhao, W.Q. Time-lag effects of global vegetation responses to climate change. *Glob. Chang. Biol.* **2015**, *21*, 3520–3531. [CrossRef]

29. Ruan, L.L.; Yan, M.; Zhang, L.; Fan, X.S.; Yang, H.X. Spatial-temporal NDVI pattern of global mangroves: A growing trend during 2000–2018. *Sci. Total Environ.* **2022**, *844*, 157075. [CrossRef]

30. Tucker, C.J.; Slayback, D.A.; Pinzon, J.E.; Los, S.O.; Myneni, R.B.; Taylor, M.G. Higher northern latitude normalized difference vegetation index and growing season trends from 1982 to 1999. *Int. J. Biometeorol.* **2001**, *45*, 184–190. [CrossRef]

31. Huemmrich, K.F.; Zesati, S.V.; Campbell, P.; Tweedie, C. Canopy reflectance models illustrate varying NDVI responses to change in high latitude ecosystems. *Ecol. Appl.* **2021**, *31*, e2435. [CrossRef] [PubMed]

32. Xu, W.X.; Liu, X.D. Response of vegetation in the Qinghai-Tibet Plateau to global warming. *Chin. Geogr. Sci.* **2007**, *17*, 151–159. [CrossRef]

33. Qu, S.; Wang, L.C.; Lin, A.W.; Zhu, H.J.; Yuan, M.X. What drives the vegetation restoration in Yangtze River basin, China: Climate change or anthropogenic factors. *Ecol. Indic.* **2018**, *90*, 438–450. [CrossRef]

34. Zhang, Y.C.S.; Du, J.Q.; Guo, L.; Sheng, Z.L.; Wu, J.H.; Zhang, J. Water conservation estimation based on time series NDVI in the Yellow River Basin. *Remote Sens.* **2021**, *13*, 1105. [CrossRef]

35. Lunetta, R.S.; Knight, J.F.; Ediriwickrema, J.; Lyon, J.G.; Worthy, L.D. Land-cover change detection using multi-temporal MODIS NDVI data. *Remote Sens. Environ.* **2006**, *105*, 142–154. [CrossRef]

36. Liang, Y. Water Environmental Capacity calculation and comprehensive water quality assessment for the Dujiangyan Reach of Mingjiang River. *Sichuan Environ.* **1996**, *15*, 59–61.

37. Guo, C.B.; Wu, R.A.; Zhang, Y.S.; Ren, S.S.; Yang, Z.H.; Li, X. Characteristics and formation mechanism of giant long-runout landslide: A case study of the Gamisi Ancient Landslide in the Upper Minjiang River, China. *Acta Geol. Sin. Engl. Ed.* **2019**, *93*, 1113–1124. [CrossRef]

38. Verhoeven, V.B.; Dedoussi, I.C. Annual satellite-based NDVI-derived land cover of Europe for 2001–2019. *J. Environ. Manag.* **2022**, *302*, 113917. [CrossRef]

39. Guo, X.Y.; Zhang, H.Y.; Wu, Z.F.; Zhao, J.J.; Zhang, Z.X. Comparison and evaluation of annual NDVI time series in China derived from the NOAA AVHRR LTDR and Terra MODIS MOD13C1 Products. *Sensors* **2017**, *17*, 1298. [CrossRef]

40. Stisen, S.; Sandholt, I.; Nørgaard, A.; Fensholt, R.; Eklundh, L. Estimation of diurnal air temperature using MSG SEVIRI data in West Africa. *Remote Sens. Environ.* **2007**, *110*, 262–274. [CrossRef]

41. Peng, S.Z.; Gang, C.C.; Cao, Y.; Chen, Y.M. Assessment of climate change trends over the Loess Plateau in China from 1901 to 2100. *Int. J. Climatol.* **2018**, *38*, 2250–2264. [CrossRef]

42. Ding, Y.X.; Peng, S.Z. Spatiotemporal trends and attribution of drought across China from 1901–2100. *Sustainability* **2020**, *12*, 477. [CrossRef]

43. Peng, S.Z.; Ding, Y.X.; Liu, W.Z.; Li, Z. 1 km monthly temperature and precipitation dataset for China from 1901 to 2017. *Earth Syst. Sci. Data* **2019**, *11*, 1931–1946. [CrossRef]

44. Peng, S.Z.; Ding, Y.X.; Wen, Z.M.; Chen, Y.M.; Cao, Y.; Ren, J.Y. Spatiotemporal change and trend analysis of potential evapotranspiration over the Loess Plateau of China during 2011–2100. *Agric. For. Meteorol.* **2017**, *233*, 183–194. [CrossRef]

45. Alcaraz-Segura, D.; Liras, E.; Tabik, S.; Paruelo, J.; Cabello, J. Evaluating the consistency of the 1982–1999 NDVI trends in the Iberian Peninsula across four time-series derived from the AVHRR Sensor: LTDR, GIMMS, FASIR, and PAL-II. *Sensors* **2010**, *10*, 1291–1314. [CrossRef]

46. Wang, Q.F.; Qi, J.Y.; Qiu, H.; Li, J.; Cole, J.; Waldhoff, S.; Zhang, X.S. Pronounced increases in future soil erosion and sediment deposition as influenced by freeze–thaw cycles in the Upper Mississippi River Basin. *Environ. Sci. Technol.* **2021**, *55*, 9905–9915. [CrossRef]

47. Wang, Q.F.; Zeng, J.Y.; Qi, J.Y.; Zhang, X.S.; Zeng, Y.; Shui, W.; Xu, Z.H.; Zhang, R.R.; Wu, X.P.; Cong, J. A multi-scale daily SPEI dataset for drought characterization at observation stations over mainland China from 1961 to 2018. *Earth Syst. Sci. Data* **2021**, *13*, 331–341. [CrossRef]

48. Wang, Q.F.; Qi, J.Y.; Li, J.; Cole, J.; Waldhoff, S.T.; Zhang, X.S. Nitrate loading projection is sensitive to freeze-thaw cycle representation. *Water Res.* **2020**, *186*, 116355. [CrossRef]

49. Zhang, Y.R.; He, Y.; Li, Y.L.; Jia, L.P. Spatiotemporal variation and driving forces of NDVI from 1982 to 2015 in the Qinba Mountains, China. *Environ. Sci. Pollut. Res.* **2022**, *29*, 52277–52288. [CrossRef]

50. Wang, Q.F.; Zhang, R.R.; Qi, J.Y.; Zeng, J.Y.; Wu, J.J.; Shui, W.; Wu, X.P.; Li, J.W. An improved daily standardized precipitation index dataset for mainland China from 1961 to 2018. *Sci. Data* **2022**, *9*, 124. [CrossRef]

51. Fensholt, R.; Proud, S.R. Evaluation of earth observation based global long term vegetation trends—Comparing GIMMS and MODIS global NDVI time series. *Remote Sens. Environ.* **2012**, *119*, 131–147. [CrossRef]

52. Ronald, E.J.; Sangermano, F.; Ghimire, B.; Zhu, H.; Chen, H.; Neeti, N.; Cai, Y.; Machado, E.A.; Crema, S.C. Seasonal trend analysis of image time series. *Int. J. Remote Sens.* **2009**, *30*, 2721–2726. [CrossRef]

53. Liu, Z.Z.; Wang, H.; Li, N.; Zhu, J.; Pan, Z.W.; Qin, F. Spatial and temporal characteristics and driving forces of vegetation changes in the Huaihe River Basin from 2003 to 2018. *Sustainability* **2020**, *12*, 2198. [CrossRef]

54. Jiang, L.L.; Guli, J.; Bao, A.M.; Guo, H.; Ndayisaba, F. Vegetation dynamics and responses to climate change and human activities in Central Asia. *Sci. Total Environ.* **2017**, *600*, 967–980. [CrossRef]

55. Cui, L.F.; Wang, L.C.; Singh, R.P.; Lai, Z.P.; Jiang, L.L.; Yao, R. Association analysis between spatiotemporal variation of vegetation greenness and precipitation/temperature in the Yangtze River Basin (China). *Environ. Sci. Pollut. Res.* **2018**, *25*, 21867–21878. [CrossRef]

56. Hou, J.; Du, L.T.; Liu, K.; Hu, Y.; Zhu, Y.G. Characteristics of vegetation activity and its responses to climate change in desert/grassland biome transition zones in the last 30 years based on GIMMS3g. *Theor. Appl. Climatol.* **2019**, *136*, 915–928. [CrossRef]

57. Weiss, J.L.; Gutzler, D.S.; Coonrod, J.E.A.; Dahm, C.N. Seasonal and inter-annual relationships between vegetation and climate in central New Mexico, USA. *J. Arid Environ.* **2004**, *57*, 507–534. [CrossRef]

58. Zhou, Y.; Zhang, L.; Fensholt, R.; Wang, K.; Vitkovskaya, I.; Tian, F. Climate contributions to vegetation variations in Central Asian Drylands: Pre- and Post-USSR collapse. *Remote Sens.* **2015**, *7*, 2449–2470. [CrossRef]

59. Zhu, M.; Zhang, J.J.; Zhu, L.Q. Article title variations in growing season NDVI and its sensitivity to climate change responses to green development in mountainous areas. *Front. Environ. Sci.* **2021**, *9*, 678450. [CrossRef]

60. Li, Y.; Yao, N.; Chau, H.W. Influences of removing linear and nonlinear trends from climatic variables on temporal variations of annual reference crop evapotranspiration in Xinjiang, China. *Sci. Total Environ.* **2017**, *592*, 680–692. [CrossRef]

61. Zamani, R.; Mirrabbasi, R.; Abdollahi, S.; Jhajharia, D. Streamflow trend analysis by considering autocorrelation structure, long-term persistence, and Hurst coefficient in a semi-arid region of Iran. *Theor. Appl. Climatol.* **2017**, *129*, 33–45. [CrossRef]

62. Yang, X.J. China's rapid urbanization. *Science* **2013**, *342*, 311. [CrossRef] [PubMed]

63. Li, J.J.; Peng, S.Z.; Li, Z. Detecting and attributing vegetation changes on China's Loess Plateau. *Agric. For. Meteorol.* **2017**, *247*, 260–270. [CrossRef]
64. Xu, Y.; Zheng, Z.W.; Guo, Z.D.; Dou, S.Q.; Huang, W.T. Dynamic variation in vegetation cover and its influencing factor detection in the Yangtze River Basin from 2000 to 2020. *Environ. Sci.* **2022**, *43*, 3730–3740.
65. Tong, X.W.; Wang, K.L.; Brandt, M.; Yue, Y.M.; Liao, C.J.; Fensholt, R. Assessing future vegetation trends and restoration prospects in the Karst Regions of Southwest China. *Remote Sens.* **2016**, *8*, 357. [CrossRef]
66. Wang, Q.; Zhang, M.J.; Wang, S.J.; Ma, Q.; Sun, M.P. Changes in temperature extremes in the Yangtze River Basin, 1962–2011. *J. Geogr. Sci.* **2014**, *24*, 59–75. [CrossRef]
67. Long, H.L.; Liu, Y.Q.; Hou, X.G.; Li, T.T.; Li, Y.R. Effects of land use transitions due to rapid urbanization on ecosystem services: Implications for urban planning in the new developing area of China. *Habitat Int.* **2014**, *44*, 536–544. [CrossRef]
68. Chen, C.; Park, T.; Wang, X.H.; Piao, S.L.; Xu, B.D.; Chaturvedi, R.K.; Fuchs, R.; Brovkin, V.; Ciais, P.; Fensholt, R.; et al. China and India lead in greening of the world through land-use management. *Nat. Sustain.* **2019**, *2*, 122–129. [CrossRef]
69. Sun, X. Vegetation Evolution Characteristics and Toughness Evaluation in Minjiang River Basin. Master's Thesis, Hebei University of Engineering, Handan, China, 2021.
70. Stow, D.; Petersen, A.; Hope, A.; Engstrom, R.; Coulter, L. Greenness trends of Arctic tundra vegetation in the 1990s: Comparison of two NDVI data sets from NOAA AVHRR systems. *Int. J. Remote Sens.* **2010**, *28*, 4807–4822. [CrossRef]
71. Sun, P.S.; Liu, S.R.; Jiang, H.; Lü, Y.L.; Liu, J.T.; Lin, Y.; Liu, X.L. Hydrologic effects of NDVI time series in a context of climatic variability in an upstream catchment of the Minjiang River. *J. Am. Water Resour. Assoc.* **2008**, *44*, 1132–1143. [CrossRef]
72. Xiong, Y.L.; Wang, H.L. Spatial relationships between NDVI and topographic factors at multiple scales in a watershed of the Minjiang River, China. *Ecol. Inform.* **2022**, *69*, 101617. [CrossRef]
73. Zhang, W.; Wang, L.C.; Xiang, F.F.; Qin, W.M.; Jiang, W.X. Vegetation dynamics and the relations with climate change at multiple time scales in the Yangtze River and Yellow River Basin, China. *Ecol. Indic.* **2020**, *110*, 105892. [CrossRef]
74. Liu, Y.X.; Liu, S.L.; Sun, Y.X.; Li, M.Q.; An, Y.; Shi, F.N. Spatial differentiation of the NPP and NDVI and its influencing factors vary with grassland type on the Qinghai-Tibet Plateau. *Environ. Monit. Assess.* **2021**, *193*, 48. [CrossRef]
75. Hou, W.J.; Gao, J.B.; Wu, S.H.; Dai, E.F. Interannual variations in growing-season NDVI and its correlation with climate variables in the Southwestern Karst Region of China. *Remote Sens.* **2015**, *7*, 11105–11124. [CrossRef]
76. Wen, Z.F.; Wu, S.J.; Chen, J.L.; Lü, M.Q. NDVI indicated long-term interannual changes in vegetation activities and their responses to climatic and anthropogenic factors in the Three Gorges Reservoir Region, China. *Sci. Total Environ.* **2017**, *574*, 947–959. [CrossRef]
77. Xu, X.Y.; Riley, W.J.; Koven, C.D.; Jia, G.S.; Zhang, X.Y. Earlier leaf-out warms air in the north. *Nat. Clim. Chang.* **2020**, *10*, 370–375. [CrossRef]
78. Ma, Q.M.; Long, Y.P.; Jia, X.P.; Wang, H.B.; Li, Y.S. Vegetation response to climatic variation and human activities on the Ordos Plateau from 2000 to 2016. *Environ. Earth Sci.* **2019**, *78*, 709. [CrossRef]
79. Zhang, Q.; Qi, T.Y.; Li, J.F.; Singh, V.P.; Wang, Z.Z. Spatiotemporal variations of pan evaporation in China during 1960–2005: Changing patterns and causes. *Int. J. Climatol.* **2015**, *35*, 903–912. [CrossRef]
80. Dietrich, C.C.; Kreyling, J.; Jentsch, A.; Malyshev, A.V. Intraspecific variation in response to magnitude and frequency of freeze-thaw cycles in a temperate grass. *AoB Plants* **2018**, *10*, plx068. [CrossRef]
81. Li, P.; Wang, J.; Liu, M.M.; Xue, Z.H.; Bagherzadeh, A.; Liu, M.Y. Spatio-temporal variation characteristics of NDVI and its response to climate on the Loess Plateau from 1985 to 2015. *Catena* **2021**, *203*, 105331. [CrossRef]
82. Zhang, Y.; Zhang, C.B.; Wang, Z.Q.; Chen, Y.Z.; Gang, C.C.; An, R.; Li, J.L. Vegetation dynamics and its driving forces from climate change and human activities in the Three-River Source Region, China from 1982 to 2012. *Sci. Total Environ.* **2016**, *563–564*, 210–220. [CrossRef]
83. Zhang, Y.L.; Song, C.H.; Band, L.E.; Sun, G.; Li, J.X. Reanalysis of global terrestrial vegetation trends from MODIS products: Browning or greening? *Remote Sens. Environ.* **2017**, *191*, 145–155. [CrossRef]
84. Jin, K.; Wang, F.; Li, P.F. Responses of vegetation cover to environmental change in large cities of China. *Sustainability* **2018**, *10*, 270. [CrossRef]
85. Liu, J.Y.; Zhang, Z.X.; Xu, X.L.; Kuang, W.H.; Zhou, W.C.; Zhang, S.W.; Li, R.D.; Yan, C.Z.; Yu, D.S.; Wu, S.X.; et al. Spatial patterns and driving forces of land use change in China during the early 21st century. *J. Geogr. Sci.* **2010**, *20*, 483–494. [CrossRef]
86. Rios, X.Z.; Brooks, P.D.; Troch, P.A.; McIntosh, J.; Guo, Q.H. Influence of terrain aspect on water partitioning, vegetation structure and vegetation greening in high-elevation catchments in northern New Mexico. *Ecohydrology* **2016**, *9*, 782–795. [CrossRef]
87. Wang, J.; Xie, Y.W.; Wang, X.Y.; Guo, K.M. Driving factors of recent vegetation changes in Hexi Region, Northwest China based on a new classification framework. *Remote Sens.* **2020**, *12*, 1758. [CrossRef]
88. Tian, H.J. Assessment of Non-Climate Triggered Vegetation Trends in China from Time Series of Remotely Sensed Data—A Case Study of Government-Dominated Forest Construction. Ph.D. Thesis, University of Chinese Academy of Sciences, Beijing, China, 2017.
89. Liu, X.F.; Zhu, X.F.; Pan, Y.Z.; Li, S.S.; Ma, Y.Q.; Nie, J. Vegetation dynamics in Qinling-Daba Mountains in relation to climate factors between 2000 and 2014. *J. Geogr. Sci.* **2016**, *26*, 45–58. [CrossRef]
90. Wang, J.; Wang, K.L.; Zhang, M.Y.; Zhang, C.H. Impacts of climate change and human activities on vegetation cover in hilly southern China. *Ecol. Eng.* **2015**, *81*, 451–461. [CrossRef]

91. Wang, J.F.; LI, H.X.; Christakos, G.; Liao, Y.L.; Zhang, T.; Gu, X.; Zhang, X.Y. Geographical detectors-based health risk assessment and its application in the neural tube defects study of the Heshun Region, China. *Int. J. Geogr. Inf. Sci.* **2010**, *24*, 107–127. [CrossRef]

92. Chen, J.; Jönsson, P.; Tamura, M.; Gu, Z.H.; Matsushita, B.; Eklundh, L. A simple method for reconstructing a high-quality NDVI time-series data set based on the Savitzky–Golay filter. *Remote Sens. Environ.* **2004**, *91*, 332–344. [CrossRef]

93. Wingate, V.R.; Phinn, S.R.; Kuhn, N. Mapping precipitation-corrected NDVI trends across Namibia. *Sci. Total Environ.* **2019**, *684*, 96–112. [CrossRef] [PubMed]

94. Roerink, G.J.; Menenti, M.; Soepboer, W.; Su, Z. Assessment of climate impact on vegetation dynamics by using remote sensing. *Phys. Chem. Earth Parts A/B/C* **2003**, *28*, 103–109. [CrossRef]

95. Braswell, B.H.; Schimel, D.S.; Linder, E.; Moore, B. The response of global terrestrial ecosystems to interannual temperature variability. *Science* **1997**, *278*, 870–872. [CrossRef]

96. Meng, X.Y.; Gao, X.; Li, S.Y.; Lei, J.Q. Spatial and temporal characteristics of vegetation NDVI changes and the driving forces in Mongolia during 1982–2015. *Remote Sens.* **2020**, *12*, 603. [CrossRef]

97. Bégué, A.; Vintrou, E.; Ruelland, D.; Claden, M.; Dessay, N. Can a 25-year trend in Soudano-Sahelian vegetation dynamics be interpreted in terms of land use change? A remote sensing approach. *Glob. Environ. Change* **2011**, *21*, 413–420. [CrossRef]

98. Piao, S.L.; Yin, G.D.; Tan, J.G.; Cheng, L.; Huang, M.; Li, Y.; Liu, R.G.; Mao, J.F.; Myneni, R.B.; Peng, S.S.; et al. Detection and attribution of vegetation greening trend in China over the last 30 years. *Glob. Chang. Biol.* **2015**, *21*, 1601–1609. [CrossRef] [PubMed]